informa
healthcare

Toll-like receptor 7 is not necessary for retroviral neuropathogenesis but does contribute to virus-induced neuroinflammation

Stephanie D Lewis,[1] Niranjan B Butchi,[1] Mohammed Khaleduzzaman,[1] Tim W Morgan,[1] Min Du,[1] Susan Pourciau,[1] David G Baker,[1] Shizuo Akira,[2] and Karin E Peterson[1]

[1]Department of Pathobiological Sciences, School of Veterinary Medicine, Louisiana State University, Baton Rouge, Louisiana, USA; and [2]Department of Host Defense, Research Institute for Microbial Diseases, Osaka University and Solution-Oriented Research for Science and Technology, Osaka, Japan

Toll-like receptor 7 (TLR7) recognizes guanidine-rich single-stranded (ss) viral RNA and is an important mediator of peripheral immune responses to several ssRNA viruses. However, the role that TLR7 plays in regulating the innate immune response to ssRNA virus infections in specific organs is not as clear. This is particularly true in the central nervous system (CNS) where microglia and astrocytes are often the first cells responding to virus infection instead of dendritic cells. In the current study, we examined the mechanism by which TLR7 contributes to ssRNA virus–induced neuroinflammation using a mouse model of polytropic retrovirus infection. The authors found that TLR7 was necessary for the early production of certain cytokines and chemokines, including CCL2 and tumor necrosis factor (TNF) and was also involved in the early activation of astrocytes. However, TLR7 was not necessary for cytokine production and astrocyte activation at later stages of infection and did not alter viral pathogenesis or viral replication in the brain. This suggests that other pathogen recognition receptors may be able to compensate for the lack of TLR7 during retrovirus infection in the CNS. *Journal of NeuroVirology* (2008) **14,** 492–502.

Keywords: retrovirus; Toll-like receptor 7; chemokines; tumor necrosis factor; brain; mouse

Introduction

Toll-like receptor 7 (TLR7) recognizes guanidine-rich single-stranded (ss) viral RNA, including vesicular stomatitis virus (VSV), human immunodeficiency virus (HIV), and influenza A (Beignon *et al,* 2005; Diebold *et al*, 2004; Heil *et al*, 2004; Lund *et al*, 2004). TLR7 is located in the endosome membrane and recognizes viral RNA from uncoating viruses, endocytosed apoptotic cellular debris, or autophagy (Lee *et al*, 2007; Wang *et al*, 2006). In the mouse, TLR7 appears to play a nonredundant role in the detection of ssRNA viruses as dendritic cells from TLR7-deficient mice did not generate an interferon alpha (IFNα) response to ssRNA viruses such as VSV and influenza (Diebold *et al*, 2004; Lund *et al*, 2004).

The role of TLR7 in regulating dendritic cell IFNα responses to ssRNA virus infection suggests that this receptor may also play a role in mediating neuroinflammatory responses to ssRNA virus infection in the central nervous system (CNS). TLR7 was only detected on ependymal cells by immunohistochemistry in the normal adult brain (Mishra *et al*, 2006). However, *Tlr7* mRNA expression has been detected in primary cultures of both astrocytes and microglia (Jack *et al*, 2005; McKimmie and Fazakerley 2005). Thus, TLR7 may contribute to the

recognition of ssRNA virus infections by microglia and astrocytes.

In the current study, we analyzed the contribution of TLR7 to ssRNA virus–induced neuroinflammatory response and neuropathogenesis, utilizing the mouse model of polytropic retrovirus infection. In this model, infection of neonatal mice with the neurovirulent polytropic retrovirus Fr98 induces severe clinical neurologic disease characterized by ataxia, seizures, and/or death by 2 to 3 weeks post infection. The effects of Fr98 infection in the CNS include viral encephalitis with associated microgliosis, mild vacuolar and neuronal degeneration, astrogliosis, and minimal mononuclear cell infiltrates (Portis et al, 1995; Robertson et al, 1997). Fr98 primarily infects CNS microglial cells, macrophages, endothelial cells, and occasionally oligodendrocytes, suggesting an indirect mechanism of neuropathogenesis (Portis *et al*, 1995; Robertson et al, 1997). One mechanism by which Fr98 may induce neuropathogenesis is through the up-regulation of proinflammatory cytokines and chemokines and the activation of astrocytes, as these responses correlate with disease (Peterson *et al*, 2001, 2004a,b). In the present study, using TLR7-deficient mice, we found that TLR7 had a significant impact on the early induction of cytokine and chemokine expression as well as astrocyte activation. However, TLR7 was not necessary for regulating retroviral replication or pathogenesis in the brain.

Results

Response of cortical cells to Fr98 infection is dependent on TLR7

TLR7 was previously shown to recognize synthetic RNAs derived from ssRNA viruses including influenza A, VSV, and HIV (Diebold *et al*, 2004; Heil et al, 2004; Lund *et al*, 2004). To examine whether TLR7 was involved in the recognition of the polytropic retrovirus Fr98, we analyzed the ability of Fr98 to stimulate primary cultures derived from the cortices of 1- to 2-day-old TLR7-sufficient and TLR7-deficient mice. These cultures were composed primarily of astrocytes, with some microglia and endothelia cells (data not shown). Stimulation with 10^4 FFU of Fr98 induced expression of interferon beta (*Ifnb1*) and *Cxcl10* (IP-10) mRNAs in cortical cultures generated from TLR7-sufficient mice (Figure 1A). In contrast, identical cultures generated from TLR7-deficient mice did not respond to Fr98 stimulation (Figure 1B). Thus, Fr98 induction of *Ifnb1* and *Cxcl10* mRNAs, *in vitro*, was dependent on TLR7.

Expression of TLR7 in the neonatal brain following Fr98 infection

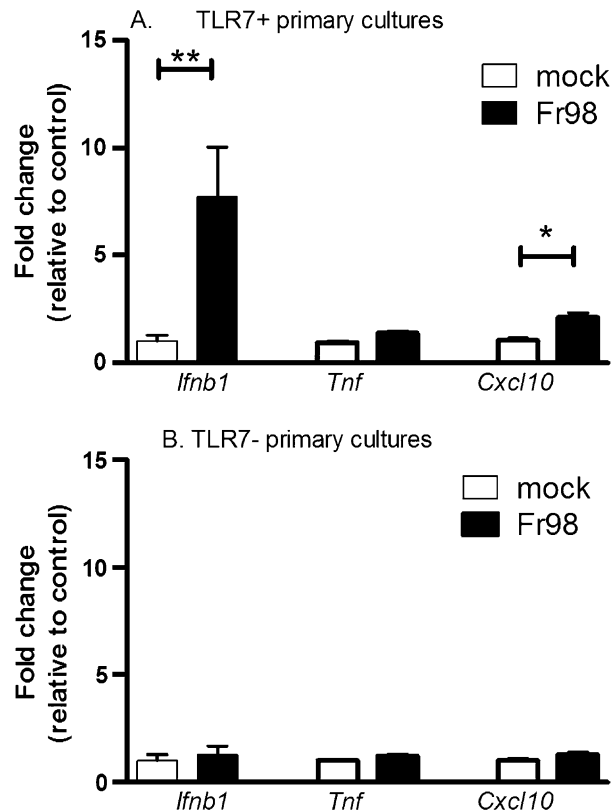Cytokine and chemokine mRNAs are induced by Fr98 infection in the CNS, with peak expression at 12

Figure 1 *In vitro* stimulation of primary cortical cultures from (**A**) TLR7-sufficient and (**B**) TLR7-deficient mice. Primary cortical cultures from (**A**) wild-type or (**B**) TLR7-deficient mice were used when cells reached approximately 80% confluency. Cultures were stimulated with 10^4 focus forming units of Fr98 or mock supernatant control in presence of 4 µg/ml of polybrene. Total RNA from the cells was extracted after 48 h using a mini RNA isolation kit (Zymo research) as per the manufacturer's instructions and analyzed for *Ifnb1, Tnf,* and *Cxcl10* mRNA expression by quantitative real-time RT-PCR. Each sample was run in triplicate. Data are the mean ± standard error for three wells per group and represent one of two experiments. Statistical analysis was done by Mann-Whitney test. Statistical significance: *$P < .05$; **$P < .01$.

to 13 days post infection (d.p.i.) (Peterson *et al*, 2001). To examine if Fr98 infection also induces *Tlr7* mRNA, we completed kinetic analysis of gene expression in the CNS, beginning at 3 d.p.i. until just prior to disease development at day 14. Virus gag RNA for Fr98 was detected in the brain at 3 d.p.i. and increased logarithmically over time (Figure 2A). *Tlr7* mRNA was up-regulated in Fr98-infected mice starting at 11 d.p.i., and remained high at 12 and 13 d.p.i. (Figure 2B). Similar kinetics were observed with *Ifnb1* and the glial fibrillary acidic protein (*Gfap*) gene, a marker of astrocyte activation (Figure 2C, D). Thus, mRNA for *Tlr7* and neuroinflammatory genes were up-regulated in a similar time frame prior to the onset of neurologic disease in Fr98-infected mice. The increase at 11 versus 3 d.p.i. suggests that a certain level of virus infection in the CNS is necessary to induce the neuroinflammatory responses.
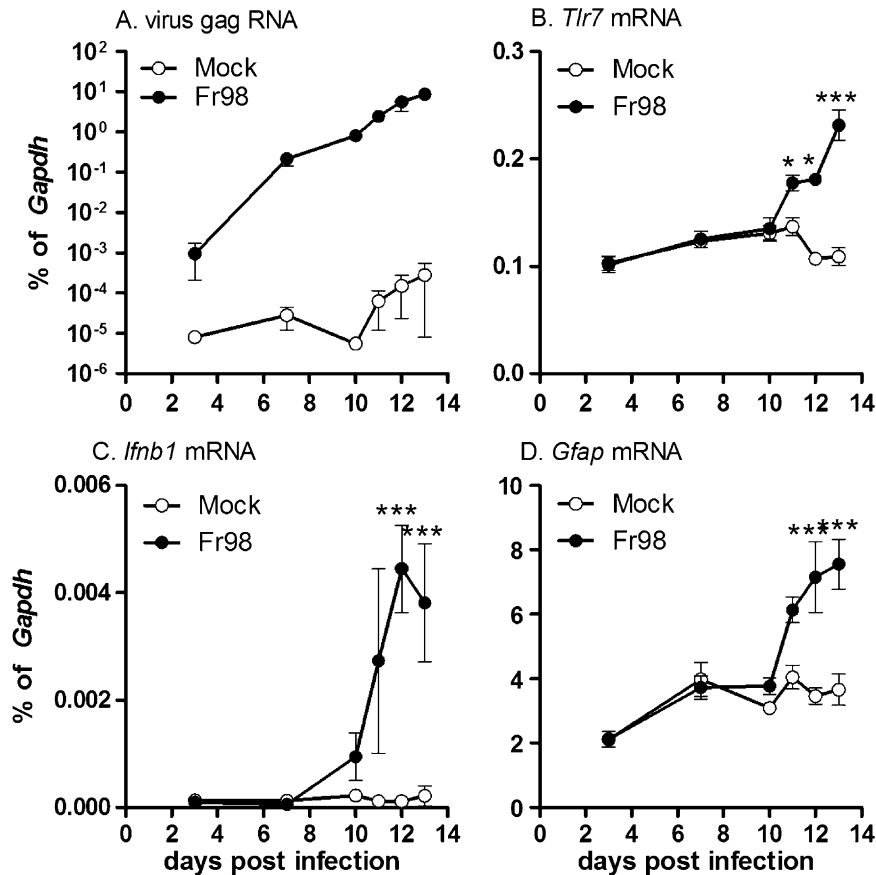
Figure 2 Kinetics of mRNA expression of neuroinflammatory genes in the brain following Fr98 infection. Brain tissues from mock- and Fr98-infected mice were removed at the time points indicated, divided into two sagittal sections and snap frozen in liquid nitrogen and processed for RNA. Real-time quantitative RT-PCR analysis was performed using primers specific for (**A**) virus gag, (**B**) *Tlr7*, (**C**) *Ifnb1*, (**D**) *Gfap* and *Gapdh*. Data were calculated as gene expression relative to *Gapdh* expression (% of *Gapdh* expression) for each sample. Data are the mean ± standard error for four mice per group. Statistical analysis was completed using a two-way ANOVA with Bonferroni post test. Statistical significance: $*P < .05$; $**P < .01$; $***P < .001$. Similar results were observed with a replicate experiment.

To determine if TLR7 cellular expression and distribution was altered following Fr98 infection, we analyzed TLR7 protein expression in brain tissue from Fr98-infected mice or uninfected controls by immunohistochemistry. TLR7 protein was observed on both virus-infected and uninfected endothelial cells (Figure 3A and B). TLR7 was not readily detected on virus-infected microglia (Figure 3C). TLR7 was detected on a population of non–virus-infected cells (Figure 3C), which were not readily observed in the mock controls, suggesting the recruitment of TLR7-positive macrophages or dendritic cells to the site of virus replication. Thus, the up-regulation of *Tlr7* mRNA associated with Fr98 infection (Figure 2B) may be due to an influx of macrophage or dendritic cells to the CNS. Alternatively, the increase in *Tlr7* mRNA expression may be due to enhanced expression of *Tlr7* mRNA by endothelial cells. Despite the infection with Fr98, neither astrocytes nor infected microglia cells appeared to up-regulate TLR7 protein expression (Figure 3C; data not shown).

Effect of TLR7 deficiency on Fr98 infection induced cytokine and chemokine production

Fr98 infection of neonates induces substantial innate immune responses, including the production of proinflammatory cytokines, as detected by both mRNA and protein expression (Peterson *et al*, 2001, 2004a, 2006; Portis *et al*, 1995; Robertson *et al*, 1997). This neuroinflammatory response peaks at approximately 12 to 14 d.p.i., prior to the onset of clinical disease (Figure 2) (Peterson *et al*, 2001, 2004a). This response includes the expression of *Ccl2* mRNA by astrocytes, *Ccl3* and *Ccl4* mRNAs by microglia, as well as *Ccl3*, *Ccl4*, and *Ccl5* mRNAs by infiltrating macrophages (Corbin *et al*, 2006; Peterson et al, 2004a; unpublished results). To determine the role of TLR7 in the innate immune response to Fr98 infection, brain tissue from 14-day-old mice was analyzed for the proinflammatory cytokines and chemokines, interleukin (IL)-12 p70, tumor necrosis factor (TNF), CCL2, CCL3, CCL4, and CCL5 by multiplex bead assay. Similar to previous reports, Fr98 infection of TLR7-sufficient mice induced a
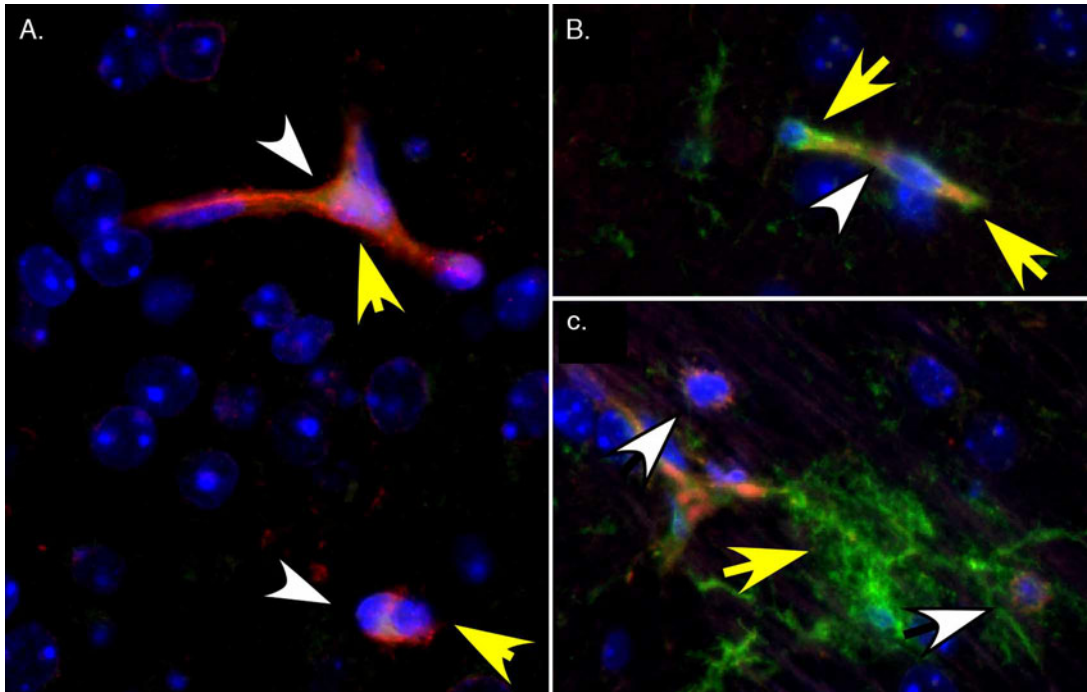
Figure 3 TLR7 protein expression in mock- (**A**) and Fr98- (**B, C**) infected mice. (**A**) CD31-positive brain capillary endothelial cells (*green fluorescence; yellow arrows*) were positive for TLR7 (*red fluorescence; white arrows*) in mock-infected mice. (**B**) Dual staining for TLR7 (*red fluorescence, white arrows*) and virus (*green fluorescence; yellow arrow*) on endothelial cells in Fr98-infected IRW mice at 14 d.p.i. (**C**) Localization of virus-infected cells (*green fluorescence; yellow arrows*) near non–virus-infected TLR7-positive cells (*red fluorescence; white arrows*). Images were from the thalamus region of the brain. Magnification was 1000 ×for **A** and B, and 400 ×for **C**.

significant up-regulation of CCL2 (monocyte chemoattractant protein [MCP]-1), CCL4 (macrophage inflammatory protein [MIP]-β), and CCL5 (RANTES) protein levels (Figure 4A to C) (Peterson *et al*, 2001, 2004b). In contrast to TLR7-sufficient mice, only CCL5 protein was up-regulated significantly by Fr98 infection in TLR7-deficient mice and this level was lower compared to TLR7-sufficient mice (Figure 4). IL-12 p70, TNF, and CCL3 protein

expression was below detection limits in all tissue samples. Because *Ccl3* and *Tnf* mRNAs have previously been shown to be up-regulated in the brain, we analyzed gene expression of these two genes, as well as *Ifnb1*, by real-time PCR. The expression of *Tnf* mRNA was significantly lower in Fr98-infected TLR7-deficient mice compared to Fr98-infected TLR7-sufficient mice (Figure 5B). However, mRNA expression of *Ccl3* and *Ifnb1* was up-regulated to
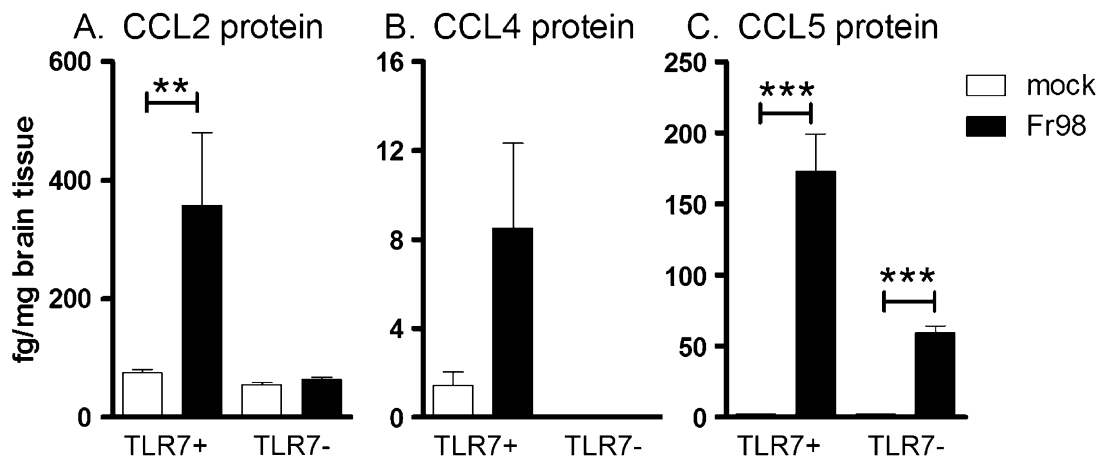

Figure 4 Influence of TLR7 deficiency on Fr98 infection–induced cytokine and chemokine protein levels in the brain. Brain tissue from mock- and Fr98-infected mice was removed at 14 d.p.i., snap frozen, and processed for multiplex bead array. Analysis of (**A**) CCL2, (**B**) CCL4, and (**C**) CCL5 protein levels in brain tissue. Results are the mean ± standard error of five to six mice per group. Data shown are from one of two replicate experiments. Statistical analysis was completed using a one-way ANOVA with Newman-Keuls post-test analysis (**P <.01; ***P <.001).
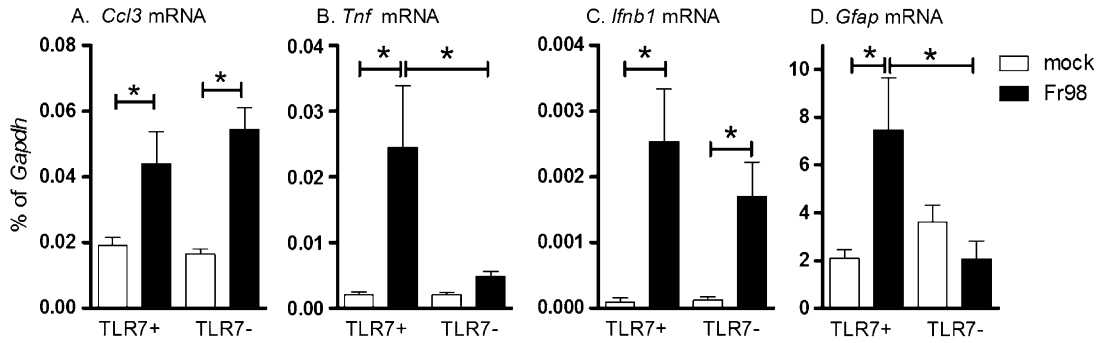
Figure 5 Influence of TLR7 deficiency on Fr98 infection–induced neuroinflammatory responses in the brain. Brain tissue from mock- and Fr98-infected mice was removed at 14 d.p.i., snap frozen, and processed for real-time PCR analysis. Expression of (**A**) *Ccl3*, (**B**) *Tnf*, (**C**) *Ifnb1*, and (**D**) *Gfap* mRNAs. Data are shown as the gene expression as a percentage of *Gapdh* mRNA expression for each sample. Results are the mean ± SEM of five to six mice per group. Data shown are from one of two replicate experiments. Statistical analysis was done by one-way ANOVA with Newman Keuls post-test analysis (*$P < .05$).

similar levels in Fr98-infected TLR7-sufficient and TLR7-deficient mice (Figure 5A, C). Thus, TLR7 was not necessary for expression of all proinflammatory cytokines and chemokines following Fr98 infection. This suggests that there are multiple pathways for the induction of innate immune responses in the CNS, with CCL2, CCL4, and TNF induced in a TLR7-specific manner, whereas other cytokines and chemokines, such as CCL3, CCL5, and IFNβ were induced utilizing other pathways.

Effect of TLR7 deficiency on Fr98 infection-induced astrocyte activation
The activation of astrocytes is one of the primary pathologic changes associated with Fr98 infection (Portis *et al*, 1995; Robertson *et al*, 1997). To examine if TLR7 was involved in Fr98 infection induced activation of astrocytes during the early stages of virus infection, we analyzed TLR7-sufficient and TLR7-deficient mice at 14 d.p.i. for mRNA expression of the astrocyte activation marker, *Gfap*. A significant increase in *Gfap* mRNA expression

was observed in Fr98-infected TLR7-sufficient mice compared to mock-infected mice (Figure 5D), similar to that observed with the kinetic analysis (Figure 2D). This increase in *Gfap* mRNA was not observed in Fr98-infected TLR7-deficient mice (Figure 5D). Thus, TLR7 appears to be required for Fr98 infection–induced astrocyte activation at 14 d.p.i.

Effect of TLR7 deficiency on Fr98-induced neurologic disease
The up-regulation of *Tlr7* mRNA during retrovirus infection and the requirement for TLR7 in the induction of several neuroinflammatory markers suggests that TLR7 may play an important role in Fr98-mediated neuropathogenesis. TLR7-sufficient and TLR7-deficient littermates were infected i.p. with Fr98 or mock culture supernatants within 24 h of birth and followed for the development of clinical disease. Surprisingly, no significant difference in the development of neurologic disease was observed between TLR7-sufficient and TLR7-deficient mice (Figure 6A). Additionally, there were no notable
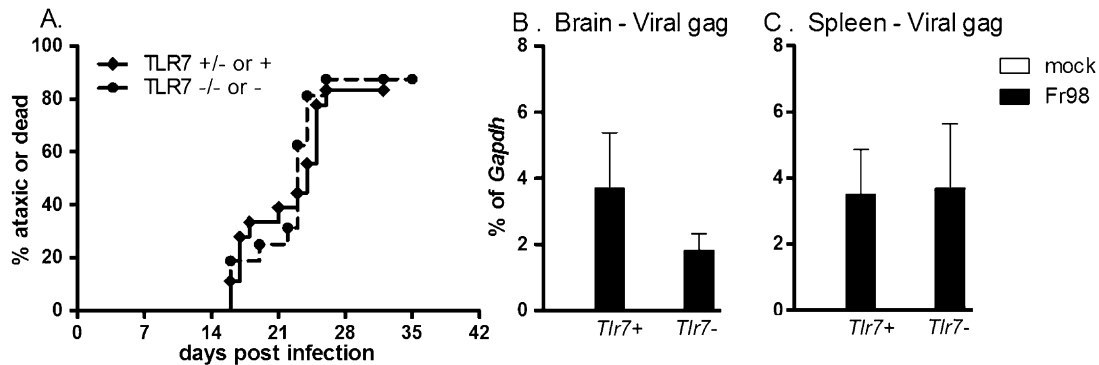

Figure 6 Analysis of the effect of TLR7 deficiency on (**A**) neurologic disease and (**B, C**) virus gag RNA expression. (**A**) Development of neurologic disease in TLR7-positive (+/− or +) and TLR7-deficient (−/− or −) Fr98-infected mice and age-matched control mice. At the time of clinical disease, mice were genotyped for TLR7-positive and knockout alleles. Data are presented as the percentage of mice with severe ataxia or dead. Data are of 14 TLR7- mice and 15 TLR7-sufficient mice. Data were analyzed using Kaplan-Meir survival curve and log-rank post test. (**B, C**) Viral gag RNA expression in (**B**) brain and (**C**) spleen tissue from mock and Fr98-infected TLR7-positive and TLR7-deficient mice at 14 d.p.i. Data are the mean ± SEM of five to six mice per group. Data shown are from one of two replicate experiments. Statistical analysis was completed using one-way ANOVA. No significant difference was observed in viral gag mRNA expression levels between TLR7-sufficient and TLR7-deficient mice.

TLR7 and retroviral neuropathogenesis
SD Lewis *et al*
497

distinctions in the histopathology of Fr98-infected TLR7-sufficient and TLR7-deficient mice as detected in H&E-stained sections or in tissue sections stained for viral envelope protein or active caspase 3 (data not shown). Thus, TLR7 did not appear to play a critical role in the development of Fr98-mediated neurologic disease. No increase in CD3 T cells was observed in either TLR7-sufficient or TLR7-deficient mice compared to mock-infected controls, consistent with previous results (Peterson et al, 2001; Robertson *et al*, 1997).

To determine if TLR7 deficiency altered virus replication during infection, we analyzed brain and spleen tissue from mock- and Fr98-infected TLR7-sufficient and TLR7-deficient mice for expression of virus gag RNA at 14 d.p.i., just prior to the development of clinical neurologic disease. No significant difference was observed in viral gag RNA expression in the brain (Figure 6B) or the spleen (Figure 6C) of Fr98-infected TLR7-sufficient mice compared to TLR7-deficient mice. Thus, TLR7 did not play a significant role in regulating virus levels in either the brain or the periphery.

Neuroinflammatory responses in clinical animals
Ccl2, *Tnf*, and *Gfap* mRNAs and/or proteins were not up-regulated in Fr98-infected TLR7-deficient mice at 14 d.p.i. (Figure 4, 5). However, progression of virus replication and the development of neurological disease may result in apoptosis of cells or release of sequestered pathogen-associated molecular patterns (PAMPs) that subsequently induce the expression of these molecules by pathways other than TLR7. Therefore, we examined brain tissue from mice with severe clinical disease (seizures and/or ataxia) for expression of *Gfap*, *Ccl2*, *Tnf*, and *Ifnb1* mRNAs by real-time PCR. Mock-infected controls were age matched to the time range at which the Fr98-infected mice developed clinical disease (2 to 5 weeks post infection). Interestingly, the influence of TLR7 on neuroinflammatory responses was not as pronounced in clinical animals as in preclinical animals. The primary example of

this was the up-regulation of *Gfap* mRNA, which was suppressed in TLR7-deficient mice at the early time point following virus infection (Figure 5D), but was not suppressed at the time of clinical disease (Figure 7A). *Tnf* mRNA levels, which were not suppressed in TLR7-deficient mice at 14 d.p.i. (Figure 5B) were significantly reduced in clinical TLR7-deficient mice compared to clinical TLR7-sufficient mice (Figure 7C). However, there was a fourfold increase in the level of *Tnf* mRNA expression in the Fr98-infected TLR7-deficient mice compared to mock-infected controls, suggesting that other pathways were contributing to *Tnf* mRNA expression (Figure 7C). Thus, TLR7 appears to play a greater role in the neuroinflammatory response during the preclinical stage of virus infection compared to the clinical stage.

Discussion

In the current study, TLR7 deficiency did not alter retroviral pathogenesis, but did alter early neuroinflammatory responses, including astrocyte activation and chemokine production. Thus, TLR7 appears to play an important role in the early glial response to virus infection, and inhibition of the pathway may reduce neuroinflammation. To date, this is the first demonstration of the role of TLR7 in neuroinflammatory responses during retrovirus infection *in vivo*.

In the neonatal brain, TLR7 was expressed in the brain capillary endothelial and ependymal cell populations (Figure 3; data not shown). Similarly, TLR7 was detected in ependymal and vascular endothelial cell populations in the adult mouse brain (Mishra *et al*, 2006). The expression of TLR7 by endothelial cells is consistent with the up-regulation of adhesion molecules in peripheral endothelia shortly after TLR7 ligand stimulation as well as immunohistochemical studies showing TLR7 expression in endothelial cells in the liver and spleen (Gunzer *et al*, 2005). The expression of
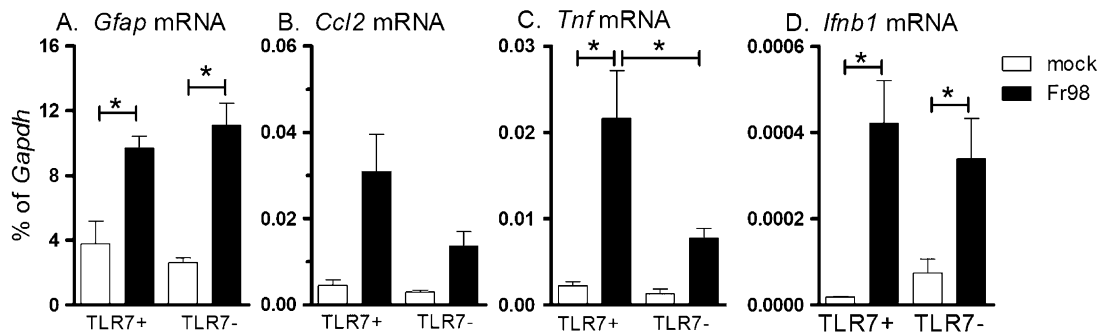
Figure 7 Expression of (**A**) *Ccl2*, (**B**) *Ifnb1*, (**C**) *Tnf*, and (**D**) *Gfap* mRNAs in the brain of Fr98-infected TLR7-positive and TLR7-deficient mice and age-matched controls at the time of apparent clinical disease (tremors, ataxia, seizures). Tissue was processed as described in Figure 5. Data are the mean ± SEM of seven to eight mice per diseased group and three mice per age-matched control group. Statistical analysis was completed using one-way ANOVA with Newman-Keuls post test analysis (*$P < .05$).

TLR7 by the ependymal cell population as well as in the endothelia of the blood-brain barrier indicates that TLR7 may play a critical role in allowing the migration of inflammatory cells into the brain following virus infection.

Microglia and astrocytes were not shown to express TLR7 protein by immunohistochemical analysis, *in vivo* (Figure 3). However, TLR7 expression was detected on these cell types in primary cultures (data not shown). The lack of TLR7 detection on microglia and astrocytes may be due to low level of expression *in vivo* that remains below the sensitivity of immunohistochemistry. Alternatively, the culturing of microglia and/or astrocytes *in vitro* may up-regulate the expression of TLR7 on these cell types.

TLR7 stimulation has been shown to both suppress and enhance HIV virus replication in peripheral blood mononuclear cells (PBMCs) (Schlaepfer *et al*, 2006). In this study, TLR7 deficiency did not alter virus replication in the brain or in the spleen, as measured by virus gag RNA expression (Figure 6). This lack of an effect may be due to the immaturity of the immune system in neonates. B cells play an important role in TLR7 mediation of HIV viral replication (Schlaepfer *et al*, 2006), and these responses are not fully developed in the neonate. Additionally, spread of Fr98 may already be restricted in the absence of an antiviral response. Fr98 infection results in a limited spread of virus to microglia/macrophages around blood vessels in the thalamus, hippocampus, corpus callosum, and cerebellum (Portis et al, 1995). Thus, other factors, such as cell cycle and/or receptor expression may influence virus infection in the brain to a greater extent than the innate immune response.

The lack of virus spread in TLR7-deficient animals may also be due to the production of IFNβ. Type 1 interferons such as IFNβ are known to suppress the spread of the virus to uninfected cells (Diebold *et al*, 2004; Heil *et al*, 2004; Kadowaki and Liu 2002; Krug *et al*, 2004; Lund *et al*, 2003). *Ifnb1* mRNA was up-regulated in response to retrovirus infection in both TLR7-sufficient and -deficient mice (Figure 5, 7) and therefore could suppress virus replication.

It is unclear why TLR7 was necessary for the *in vitro* IFNβ response to Fr98 but not the *in vivo* response. In the *in vitro* cultures, Fr98 stimulation was not via a productive infection, but rather due to the ability of cells to take up virus particles. There is also no potential conditioning of responding cells through the production of other cytokines, apoptotic cells, or infiltrating cells. The environmental factors of other cytokines, apoptotic cells, as well as a highly productive virus infection, *in vivo*, may circumvent the need for TLR7 for the induction of IFNβ. For example, in the microenvironment of infected microglia cells, there may be a very high level of virus envelope protein expression on the

cell surface. TLR4 has been shown to be activated by retroviral envelope glycoproteins and can induce the expression of *Ifnb1* (Burzyn *et al*, 2004). Thus, TLR4 stimulation by Fr98 envelope proteins may be sufficient for the induction of *Ifnb1* mRNA in the absence of TLR7, *in vivo*.

Despite the lack of effect on virus replication and clinical disease in this model, TLR7 deficiency had a significant impact on early neuroinflammatory responses. Many, but not all, chemokines were reduced and cellular responses were also limited. Similar suppression of the innate immune response was observed with TLR2-deficient mice following herpes simplex virus (HSV)-1 infection (Kurt-Jones *et al*, 2004). Mice deficient in TLR3 had reduced infiltration of virus and immune cells to the brain following West Nile virus infection (Wang *et al*, 2004). Thus, specific TLRs may play critical non-overlapping roles in the initiation of immune responses to certain viruses.

The requirement for TLR7 in Fr98-mediated up-regulation of multiple cytokines and chemokines in preclinical animals was surprising, as many of these cytokine- and chemokine-producing cells are not productively infected with virus. For example, *Ccl2* and *Cxcl10* mRNAs are produced by astrocytes, which are not infected by Fr98 (Peterson *et al*, 2004a; Robertson *et al*, 1997) (data not shown). As several of the chemokine secreting cell types are not productively infected by Fr98, it is unclear how TLR7 influences their response to virus infection. Possibly, these cells are not directly activated through TLR7 signaling, but are responding to a secreted cytokine or other signaling molecule produced by an infected cell. This response may be inhibited in the absence of TLR7. Alternatively, astrocytes and other uninfected cell types may take up viral particles, including viral ssRNA by phagocytosis, leading to the activation of these cells through TLR7.

The lack of *Gfap* mRNA up-regulation in TLR7-deficient preclinical animals was consistent and significant in multiple experiments (Figure 5D). However, in the clinical animals, *Gfap* mRNA was up-regulated to levels consistent with wild-type mice (Figure 7A). This difference may be due to changes in the microenvironment between preclinical and clinical animals. It is also possible that the astrocyte response in TLR7-deficient mice at the time of clinical disease is a response to disease pathogenesis rather than a direct response to virus infection.

Other Toll-like receptors may also influence inflammatory responses to retrovirus infection. ssRNA genomes activate TLR7 (Diebold *et al*, 2004, Heil *et al*, 2004) whereas TLR9 recognizes CpG DNA (Bauer *et al*, 2001, Hemmi *et al*, 2000, Lund et al, 2003). During HIV infection, HIV-1 RNA, rather than DNA retroviral transcripts, appears to be essential for activating plasmacytoid dendritic cells (Beignon

TLR7 and retroviral neuropathogenesis
SD Lewis et al
499

et al, 2005). However, TLR9 polymorphisms were shown to substantially influence rapid progression of acquired immunodeficiency syndrome (AIDS) (Bochud *et al*, 2007). Thus, both TLR7 and TLR9 may influence retroviral pathogenesis. In the current study, TLR9 may be stimulated by Fr98 viral CpG DNA released into the cellular environment by infected apoptotic cells. Therefore, the neuropathogenesis induced in Fr98-infected mice may be a combination of responses to TLR7 and TLR9, and not solely due to TLR7.

Materials and methods

Mice
Tlr7-deficient C57BL/6 mice (Hemmi *et al*, 2002) were backcrossed with Inbred Rocky Mountain White (IRW) mice for eight generations prior to use. The *Tlr7* gene is located on the X chromosome. To generate litters containing 50% *Tlr7*-sufficient ($+/-$ or $+$) and 50% *Tlr7*-deficient ($-/-$ or $-$) mice, *Tlr7*-deficient males were mated with *Tlr7* heterozygous females. All mice were maintained at the Louisiana State University School of Veterinary Medicine. All animal experiments were conducted in accordance with the regulations of the Louisiana State University Institutional Animal Care and Use Committee.

Genotyping for Tlr7 wild-type and knockout alleles
DNA was isolated from individual mouse tail biopsies using Sigma GenElute Mammalian Genomic DNA Miniprep Kit (Sigma Aldrich, St. Louis, MO) following the manufacturer's instructions. Detection of both wild-type and knockout alleles were completed in the same polymerase chain reaction (PCR) reaction using the *Tlr7* forward primer TCCAGTGT-CATGCCTACCTGT in combination with the *Tlr7* wild-type primer GGCGGTCAGAGGATAACTTGT and the *Tlr7* knockout primer ATGCCTGCTTGCC-GAATATC. Products were amplified under the following conditions: 94°C for 3 min, followed by 25 cycles of 94°C for 30 s, 60°C for 30 s, and 70°C for 30 s, and then 72°C for 10 min. Wild-type alleles generated a 250-bp band, and knockout alleles produced a 450-bp band. mRNA expression of *Tlr7* correlated with the *Tlr7* $+/-,+$ and $-/-, -$ genotypes.

Virus infection of mice
The construction of virus clone Fr98 has been previously described (Portis *et al*, 1995). Virus stocks were prepared from the supernatant of Fr98- or mock-infected *Mus dunni* fibroblast cell cultures. Envelope-specific monoclonal antibodies 514 and 720 were used in focus forming assays to determine virus titers (Robertson *et al*, 1991). Virus stocks were stored at $-80°C$ until use. Newborn IRW mice were infected intraperitoneally (i.p.) with 100 µl of cell culture supernatant from mock-infected cells or 10^4 focus-forming units (FFU) of Fr98 virus within 24 h of birth. Mice were either euthanized at day 14 post inoculation prior to development of clinical disease or allowed to progress past day 14 and develop clinical signs of disease. Mice were euthanized at day 14 post inoculation as that is when peak cytokine and chemokine response is observed (Peterson *et al*, 2001). Mice that were allowed to progress past day 14 were observed daily for clinical signs of CNS disease, which include ataxia and/or seizures (Portis *et al*, 1995). Mice were immediately euthanized at the observed onset of clinical signs of disease, because clinical development of disease is rapid and can result in a moribund condition within a 24-h time period.

Histological analysis
Hemisected brain tissue samples were immersion fixed in 10% neutral-buffered formalin for 48 h, embedded in paraffin, and cut in 4-µm paracentral sagittal sections that included cerebrum, cerebellum, and brainstem. Tissue sections were adhered to coated microscope slides and stained with hematoxylin and eosin (H&E) using an automated histological stainer. Additional tissue samples were stained with antibodies to virus envelope, CD3 (Dako, Carpinteria, CA), or active caspase 3 (Promega, Madison, WI) as described below. Slides were examined in a blind fashion for histopathological evidence of neuroinflammation and neurodegeneration.

Immunohistochemical analysis
Sections were incubated twice in xylene for 15 min to remove residual paraffin and rehydrated with 5-min incubations in 100%, 95%, and 70% ethanol, and twice in phosphate-buffered saline (PBS). Antigen retrieval was performed using sodium citrate antigen retrieval buffer in a decloaking chamber (Biocare Medical, Concord, CA) set at 120°C for 20 min and cooled to 90°C. Samples were then rinsed $4 \times$ in ultrapure water and washed twice with 0.2% fish skin gelatin (FSG) (Sigma Aldrich, St. Louis, MO)/PBS (0.2% FSG/PBS) for 10 min. Slides were incubated in 1% normal donkey serum for 30 min in a humidity chamber (Evergreen Scientific, Los Angeles, CA). Slides were then incubated overnight at 4°C with primary antibody. TLR7 antigen was detected using a polyclonal rabbit anti-TLR7 antibody (Zymed, Carlsbad, CA), with biotinylated goat anti-rabbit secondary antibody and streptavidin-conjugated to AlexaFluor 555 (Invitrogen, Carlsbad, CA). CD31 was detected using a goat polyclonal antibody to mouse CD31 antibody and a rabbit anti-goat antibody conjugated to AlexaFluor 488 (Invitrogen). Goat anti-virus gp70 was detected using a rabbit anti-goat antibody conjugated to AlexaFluor 488 (Invitrogen). Secondary antibodies were applied at a dilution of 6.67 µg/ml in 0.2% FSG/PBS and

incubated for at least 30 min at room temperature. All sections were counterstained with DAPI at a concentration of 100 ng/ml. Slides were rinsed twice in 0.2% FSG/PBS. Slides were mounted with ProLong Gold anti-fade reagent (Invitrogen) and allowed to set for at least 2 h at 4°C. An irrelevant rabbit anti-mouse immunoglobulin G (Ig) antibody did not produce detectable fluorescence. Images were pseudocolored and overlayed using ImagePro Plus software.

Mutiplex assay for chemokine expression
Infected and control mice were placed under deep isoflurane anesthesia and exsanguinated via cardiac puncture followed by cervical dislocation. Brain tissue was then divided by mid-sagittal dissection into two pieces. Tissue sections were frozen in liquid nitrogen and stored at -80°C. Tissue homogenates were generated for analysis by weighing samples and homogenizing them in 400 μl of Bio-Plex cell lysis solution (Bio-Rad Laboratories, Hercules, CA) containing Complete Mini protease inhibitors (Roche Applied Science, Indianapolis, IN) and 2 mM phenylmethylsulfonyl fluoride (Sigma Aldrich). Samples were homogenized using Kontes Disposable Pellet Pestles (Fisher Scientific, Hampton, NH) and diluted to 400 μg/ml in lysis buffer. Centrifugation at $4500 \times g$ for 15 min at 4°C removed cellular debris. Cytokine protein expression was analyzed using a Cytokine 6-plex assay (BioSource, Camarillo, CA) on a Bio-Plex instrument (Bio-Rad) following manufacturer's instructions. Samples were calculated as pg/ml using a standard curve from in-plate standards and subsequently converted to fg/mg of brain tissue.

Preparation of RNA for real-time PCR analysis
Total RNA was isolated from brain tissue using Trizol reagent (Invitrogen), and samples were subsequently treated with DNase (Ambion, Austin, TX) for 30 min. Samples were then purified over Zymo RNA Cleanup Columns (Zymo Research, Orange, CA), and the RNA was reverse transcribed using iScript Reverse Transcription kit (Bio-Rad) following manufacturer's instructions. Following the reverse transcriptase reaction, samples were diluted fourfold in RNase-free water prior to use in real-time PCR reactions.

Real-time PCR analysis of gene expression
Primers for real-time PCR analysis are shown in Table 1. All primers used for real-time analysis were designed using Primer3 software (Rozen and Skaletsky, 2000). Primer sequences were blasted against the National Center for Biotechnology Information (NCBI) database to confirm that all primer pairs were specific for the gene of interest and that no homology to other genes was present. Reactions were run using SYBR green mix with Rox (Bio-Rad) in a 10-μl volume with approximately 10 ng of cDNA and 1.8 μM forward and reverse primers. Samples were run in triplicate on an ABI PRISM 7900 Sequence Detection System (Applied Biosystems, Foster City, CA). Analysis of dissociation curves was used to confirm the amplification of a single product for each primer pair per sample. Confirmation of a lack of DNA contamination was achieved by analyzing samples that had not undergone reverse transcription. Untranscribed controls had at least a 1000-fold lower expression level than analyzed samples or were negative for all genes after 40 cycles. Gene expression was quantified by the cycle number at which each sample reached a fixed fluorescence threshold (C_T). To control for variations in RNA amounts among samples, data were calculated as the difference in C_T values ($\log_2$) between *Gapdh* and the gene of interest for each sample ($\triangle C_T = C_T$ Gapdh $- C_T$ gene of interest). Data are presented as a percentage of *Gapdh* expression for each gene of interest.

Table 1 List of primers used for real-time PCR analysis

Common gene name	NCBI gene symbol and ID no.	Forward primer	Reverse Primer
Actin	*Actb*: 11461	CAGCTTCTTTGCAGCTCCTT	CACGATGGAGGGGAATACAG
Chemokine ligand 2 (MCP-1)	*Ccl2*: 20296	TCCCAATGAGTAGGCTGGAG	CCTCTCTCTTGAGCTTGGTGA
Chemokine ligand 3 (MIP-1a)	*Ccl3*: 20302	ACCATGACACTCTGCAACCA	GATGAATTGGCGTGGAATCT
Chemokine ligand 4 (MIP-1)	*Ccl4*: 20303	AGTCCCAGCTCTGTGCAAAC	CCACGAGCAAGAGGAGAGAG
Chemokine ligand 5 (RANTES)	*Ccl5*: 20304	GGTTTCTTGATTCTGACCCTGTA	AGGACCGGAGTGGGAGTAG
Chemokine ligand 10 (IP10)	*IP10*: 15945	CAGTGAGAATGAGGGCCATAGG	CTCAACACGTGGGCAGGAT
Friend murine leukemia virus Fb29 gag (gag)	*gag*: 1491876	AAACCAATGTGGCCATGTCATT	AAATCTTCTAACCGCTCTAACTTTCG
Glyceraldehyde-3-phosphate dehydrogenase (Gapdh)	*Gapdh*: 407972	TGCACCACCAACTGCTTAGC	TGGATGCAGGGATGATGTTC
Glial fibrillary acidic protein (GFAP)	*Gfap*: 14580	CGTTTCTCCTTGTCTCGAATGAC	TCGCCCGTGTCTCCTTGA
Interferon beta (Ifnb1)	*Ifnb1*: 15977	AGCACTGGGTGGAATGAGAC	TCCCACGTCAATCTTTCCTC
Toll-like receptor 7	*Tlr7*: 170743	GGCATTCCCACTAACACCAC	TTGGACCCCAGTAGAACAGG
Tumor necrosis factor alpha (Tnf)	*Tnf*: 21926	CCACCACGCTCTTCTGTCTAC	GAGGGTCTGGGCCATAGAA

TLR7 and retroviral neuropathogenesis
SD Lewis *et al*
501

Preparation of primary cortical cultures
Primary cultures were generated from the cortical tissue of 1- to 2-day-old neonatal IRW mice. When mice were less than 48 h of age, intact brains were removed and dissected free of meninges and blood vessels to prevent contamination by fibroblasts. The midbrain and cerebellum were removed and the cortices were broken down by pipeting gently in PBS/2% glucose and incubated at 37°C for 10 min. Cells were pelleted at $194 \times g$ for 5 min, and a single-cell suspension was made by triturating with a 1-ml syringe/20-G needle. Cells were cultured in 25-cm^2 Primaria tissue culture flasks (BD Bioscience) in Dulbecco's modified Eagle's medium (DMEM) with 10% fetal bovine serum (FBS), 4 mM l-glutamine, 4.5 g/L glucose, and sodium pyruvate for 10 days, then trypsinized and replated in 12-well plates for analysis. When cell reached approximately 80% confluency in the well, they were stimulated with Fr98 virus (10^4 FFU) or mock culture supernatants in presence of 4 μg/ml of polybrene in DMEM. At 48 h post stimulation, total RNA from the cells was extracted using Zymo RNA isolation kits.

Statistical analysis
All statistical analyses were performed using Graph-Pad Prism software (San Diego, CA) using the appropriate statistical test. Mann-Whitney analysis was utilized when comparing only two groups. One-way analysis of variance (ANOVA) analysis with a Newman-Keuls correction was utilized when comparing more than two groups at one time point. A two-way ANOVA with a Bonferroni post-test was utilized for kinetic analysis. Survival curve analysis was used to determine significant differences in disease development between the two strains. Indications of statistical significance are $*P < .05$; $**P < .01$; $***P < .001$.

References

Bauer S, Kirschning CJ, Hacker H, Redecke V, Hausmann S, Akira S, Wagner H, Lipford GB (2001). Human TLR9 confers responsiveness to bacterial DNA via species-specific CpG motif recognition. *Proc Natl Acad Sci USA* **98:** 9237–9242.

Beignon AS, McKenna K, Skoberne M, Manches O, DaSilva I, Kavanagh DG, Larsson M, Gorelick RJ, Lifson JD, Bhardwaj N (2005). Endocytosis of HIV-1 activates plasmacytoid dendritic cells via Toll-like receptor-viral RNA interactions. *J Clin Invest* **115:** 3265–3275.

Bochud PY, Hersberger M, Taffe P, Bochud M, Stein CM, Rodrigues SD, Calandra T, Francioli P, Telenti A, Speck RF, Aderem A (2007). Polymorphisms in Toll-like receptor 9 influence the clinical course of HIV-1 infection. *AIDS* **21:** 441–446.

Burzyn D, Rassa JC, Kim D, Nepomnaschy I, Ross SR, Piazzon I (2004). Toll-like receptor 4-dependent activation of dendritic cells by a retrovirus. *J Virol* **78:** 576–584.

Corbin ME, Pourciau S, Morgan TW, Boudreaux M, Peterson KE (2006). Ligand up-regulation does not correlate with a role for CCR1 in pathogenesis in a mouse model of non-lymphocyte mediated neurological disease. *J NeuroVirol* **12:** 1–10.

Diebold SS, Kaisho T, Hemmi H, Akira S, Reis e Sousa (2004). Innate antiviral responses by means of TLR7-mediated recognition of single-stranded RNA. *Science* **303:** 1529–1531.

Gunzer M, Riemann H, Basoglu Y, Hillmer A, Weishaupt C, Balkow S, Benninghoff B, Ernst B, Steinert M, Scholzen T, Sunderkotter C, Grabbe S (2005). Systemic administration of a TLR7 ligand leads to transient immune incompetence due to peripheral-blood leuko-cyte depletion. *Blood* **106:** 2424–2432.

Heil F, Hemmi H, Hochrein H, Ampenberger F, Kirschning C, Akira S, Lipford G, Wagner H, Bauer S (2004). Species-specific recognition of single-stranded RNA via toll-like receptor 7 and 8. *Science* **303:** 1526–1529.

Hemmi H, Kaisho T, Takeuchi O, Sato S, Sanjo H, Hoshino K, Horiuchi T, Tomizawa H, Takeda K, Akira S (2002). Small anti-viral compounds activate immune cells via the TLR7 MyD88-dependent signaling pathway. *Nat Immunol* **3:** 196–200.

Hemmi H, Takeuchi O, Kawai T, Kaisho T, Sato S, Sanjo H, Matsumoto M, Hoshino K, Wagner H, Takeda K, Akira S (2000). A Toll-like receptor recognizes bacterial DNA. *Nature* **408:** 740–745.

Jack CS, Arbour N, Manusow J, Montgrain V, Blain M, McCrea E, Shapiro A, Antel JP (2005). TLR signaling tailors innate immune responses in human microglia and astrocytes. *J Immunol* **175:** 4320–4330.

Kadowaki N, Liu YJ (2002). Natural type I interferon-producing cells as a link between innate and adaptive immunity. *Hum Immunol* **63:** 1126–1132.

Krug A, Luker GD, Barchet W, Leib DA, Akira S, Colonna M (2004). Herpes simplex virus type 1 activates murine natural interferon-producing cells through toll-like receptor 9. *Blood* **103:** 1433–1437.

Kurt-Jones EA, Chan M, Zhou S, Wang J, Reed G, Bronson R, Arnold MM, Knipe DM, Finberg RW (2004). Herpes simplex virus 1 interaction with Toll-like receptor 2 contributes to lethal encephalitis. *Proc Natl Acad Sci U S A* **101:** 1315–1320.

Lee HK, Lund JM, Ramanathan B, Mizushima N, Iwasaki A (2007). Autophagy-dependent viral recognition by plasmacytoid dendritic cell. *Science* **315:** 1398–1401.

Lund J, Sato A, Akira S, Medzhitov R, Iwasaki A (2003). Toll-like receptor 9-mediated recognition of Herpes simplex virus-2 by plasmacytoid dendritic cells. *J Exp Med* **198:** 513–520.

Lund JM, Alexopoulou L, Sato A, Karow M, Adams NC, Gale NW, Iwasaki A, Flavell RA (2004). Recognition of single-stranded RNA viruses by Toll-like receptor 7. *Proc Natl Acad Sci USA* **101:** 5598–5603.

McKimmie CS, Fazakerley JK (2005). In response to pathogens, glial cells dynamically and differentially regulate Toll-like receptor gene expression. *J Neuroimmunol* **169:** 116–125.

Mishra BB, Mishra PK, Teale JM (2006). Expression and distribution of Toll-like receptors in the brain during murine neurocysticercosis. *J Neuroimmunol* **181:** 46–56.

Peterson KE, Errett JS, Wei T, Dimcheff DE, Ransohoff R, Kuziel WA, Evans L, Chesebro B (2004a). MCP-1 and CCR2 contribute to non-lymphocyte-mediated brain disease induced by Fr98 polytropic retrovirus infection in mice: role for astrocytes in retroviral neuropathogenesis. *J Virol* **78:** 6449–6458.

Peterson KE, Evans LH, Wehrly K, Chesebro B (2006). Increased proinflammatory cytokine and chemokine responses and microglial infection following inoculation with neural stem cells infected with polytropic murine retroviruses. *Virology* **354:** 143–153.

Peterson KE, Hughes S, Dimcheff DE, Wehrly K, Chesebro B (2004b). Separate sequences in a murine retroviral envelope protein mediate neuropathogenesis by complementary mechanisms with differing requirements for tumor necrosis factor alpha. *J Virol* **78:** 13104–13112.

Peterson KE, Robertson SJ, Portis JL, Chesebro B (2001). Differences in cytokine and chemokine responses during neurological disease induced by polytropic murine retroviruses Map to separate regions of the viral envelope gene. *J Virol* **75:** 2848–2856.

Portis JL, Czub S, Robertson S, McAtee F, Chesebro B (1995). Characterization of a neurologic disease induced by a polytropic murine retrovirus: evidence for differential targeting of ecotropic and polytropic viruses in the brain. *J Virol* **69:** 8070–8075.

Robertson MN, Miyazawa M, Mori S, Caughey B, Evans LH, Hayes SF, Chesebro B (1991). Production of monoclonal antibodies reactive with a denatured form of the Friend murine leukemia virus gp70 envelope protein: use in a focal infectivity assay, immunohistochemical studies, electron microscopy and western blotting. *J Virol Methods* **34:** 255–271.

Robertson SJ, Hasenkrug KJ, Chesebro B, Portis JL (1997). Neurologic disease induced by polytropic murine retroviruses: neurovirulence determined by efficiency of spread to microglial cells. *J Virol* **71:** 5287–5294.

Rozen S, Skaletsky HJ (2000). Primer3 on the WWW for general users and for biologist programmers. Bioinformatics Methods and Protocols. *Methods Mol Biol* **132:** 365–386.

Schlaepfer E, Audige A, Joller H, Speck RF (2006). TLR7/8 triggering exerts opposing effects in acute versus latent HIV infection. *J Immunol* **176:** 2888–2895.

Wang JP, Liu P, Latz E, Golenbock DT, Finberg RW, Libraty DH (2006). Flavivirus activation of plasmacytoid dendritic cells delineates key elements of TLR7 signaling beyond endosomal recognition. *J Immunol* **177:** 7114–7121.

Wang T, Town T, Alexopoulou L, Anderson JF, Fikrig E, Flavell RA (2004). Toll-like receptor 3 mediates West Nile virus entry into the brain causing lethal encephalitis. *Nat Med* **10:** 1366–1373.